Szent István University

PRODUCTION OF NANOSTRUCTURED FERRITE RAW MATERIALS WITH MECHANICAL MILLING

Thesis of the doctoral (Ph.D.) dissertation

Gyula Kakuk

Gödöllő
2009

CONTENTS

1. INTRODUCTION AND AIMS OF THE DOCTORAL DISSERTATION

1.1. The significance of the research

Nanotechnologies are methods that form products that are smaller than 100 nanometers. The significant interest from the side of the scientific life for nanomaterials is because in the scale under 100 nanometres the materials block characteristics change and new, previously not known characteristics (strength, magnetic, etc.) can appear. There are several possible ways nowadays to create nanostructure materials from the classical and/or newly developed technologies of the material science. During these procedures the size, structure, composition and morphological features of the grains and/or phases can be changed by changing the technological parameters. One of the possible procedures is the mechanical milling that is applied for producing powders for decades. The development results of the different type of mills (for example the higher energy input than before) made it possible to produce nanocrystallic powder material. For the planned milling and the ensuring of the quality of the material that should be produced, it is essential to have a more controllable milling procedure. The mills break-up the grains in different ways, according to their operation principles, so the kinetics of the procedure is different too. The modelling of the processes that are in the planetary ball mills applied in the thesis has been studied by several researchers, but for the different milling tasks there are no exact information in the literature that is about the relation between milling parameters that controls the procedure and the delivered energy to the material to be milled. Considering this fact, the further clearance of the process that takes place inside the planetary ball mill and the exploration of the effects of the milling parameters is justified.

In the field of technical sciences, nowadays the development of the different magnetic materials are specially considered. One of the main group of the magnetic ceramics are the ferrites, that are used in several fields because of their advantageous magnetic characteristics. The ferrite dielectric systems are used for communication technological parts that work on millimeter wavelength. The use of these is very widespread, for example: broadband wireless connections, point-to-point connected microwave radios, point-multipoint connections in business and public fields (mobil communication), satellite based communication technologies, radars in automotive fields, etc.

With the improvement of the communication technology, that is with the improvement of the frequency, the ferrite device decreases, so the size of the ferrite material inside them also decreases and the role of the chemical and morphological homogeneity becomes more and more important. Only a few ferrite material system is suitable for fulfilling the increasing requirements. This is the reason why in passive microwave devices over 40 GHz, only one type of material system is applicable, the hexagonal ferrites. The great anisotropy of hexaferrites matches with a great magnetic saturation value, so these materials are perfect for producing self-bias, miniaturized component parts. But with this construction the hexaferrite must be an excellent permanent magnet too, besides having good microwave parameters. The basic condition of this that it's magnetic anisotropy must be high, which can only be reached with a well oriented structure. Hexagonal ferrites with great magnetic anisotropy can only be produced from onedomain grain sized, presintered ferrite-powder, but for this, powder with grain size less than 1µm is needed. This grain size is impossible to produce with conventional ceramic technology. This can only be done with a method that is different from the conventional ceramic technology, with a so-called „non-conventional" technic (for example: high energy milling or sol-gel technology, etc.), that leads to hexagonal ferrites with great magnetic anisotropy, little magnetic and dielectric loss, low temperature depending magnetic saturation.

The appliance of nano technologies during the production of ferrite materials can only be found in laboratory circumstances. The first scientific publications were published in Bordeaux in 1997, at the International Conference of Ferrites. Beyond the reduction of the previously mentioned grain size that is critical for the usage, the other economical advantage of the nano technologies is that the reactivity of the material increases with the decreasing of the grain size. This probably leads to the decreasement of the temperature and energy need of sintering. The one domain nano grains have

greater magnetic moment than the materials that were produced with the conventional powder metallurgy that have the same chemical composition. Nowadays the different nano technological methods compete with each other.

1.2. The aims of the research

During my work the aim of the research was to model the graining procedure that is inside the planetary ball mill and produce a certain composition of W-type barium-hexaferrite with higher energy mechanical milling than the conventional. My goal was to find new results for the description of the milling process that can be used commonly for engineering and material science practice (mechanical milling, mechanochemistry, mechanical alloying), and to apply these knowledge on a definite material system, the hexaferrites. During my research I have achieved the following main aims and tasks:

- Valued and summarized the main scientific results of modelling mechanical milling with planetary ball mills based on a unified aspect;

- Determined the main characteristics that affect the milling and the effectiveness of the milling (kinetic energy) so they can be the leader parameters of the process;

- Developed a calculation model to determine the kinetic energy, that is integrated and is able to simulate the milling process in a planetary ball mill within a domain of variability;

- Performed mechanical milling experiments during the producing of a certain ceramic material system (W-type Ba-hexaferrite) that discover the technological changes of the steps during the process with up to date material testing method as the followings:

  a) The systematic mechanical milling of the basic materials for the ferrite production (Fe_2O_3, $BaCO_3$, ZnO, $NiCO_3$) to determine the effect of the different components to each other during milling and the grindability of the basic materials.

  b) Finding that are there additives or medium that can improve the effectiveness of the milling during adverse conditions (for example: agglomeration), considering that these milling effectiveness improving additives can affect the whole technology and the steps of the production of the hexaferrite.

  c) Systematic mechanical milling of the premixed base materials that contain all the components according to the structure and stoichiometry of the needed end product and producing W-type Ba-hexaferrite from that to answer the question if it is possible to create new characteristics by mixing powders with different grain sizes (micro and/or nano grinds). This goal needed the classification of the magnetic and microstructural characteristics of the produced material (for example: structure, morphology, magnetic and dielectric properties) and the searching of the relation between the grain size and the reached characteristics.

2. MATERIAL AND METHOD

2.1. Modelling the milling process of a planetary ball mill

At the beginning of the kinetic modelling of the milling process I started from the statement that the detachment of the milling ball from the wall of the vial, can only happen when the effecting force that points to the radius of the vial is zero. I have applied the following assumptions that simplify the modelling of the planetary ball mill:

(a) The new meeting point of the ball and the vial acts as an impact point, inobservance the elastic collision of the ball (I considered the vial and the ball as inelastic bodies).

(b) There is no relative movement (slip) between the ball and the wall of the vial, before the detachment point.

(c) The resistance of the medium in the vial is discarded.

(d) I do not consider the gravity that affects the ball (perpendicular to the observed plane).

(e) I do not consider the occurrent spinning of the ball.

(f) The model is elaborated to a mill with inner diameter 65 mm, volume vial 80 ml and ball diameter 10 mm.

The steps of the modelling were the followings:

- ➢ description of the movement and force conditions
- ➢ determining the detachment angle
- ➢ determining the detachment speed
- ➢ determining the impacting point
- ➢ determining the impacting speed
- ➢ determining the action energy and output
- ➢ drawing the curve of the work of the planetary ball mill.

2.1.1. The kinetic modelling of the milling process

I have made the determination of the forces that affect the milling ball according to the work of Lü and Lai from 1998. After check-counting I have found this calculation to be a good starting point to the model that I wanted to set up.

In ball mill the milling vial is orbiting. The two (in some cases four) milling vials with a radius r_v takes place on the sun disk of a constant r_p distance from point O, and spinning around it with a ω_p angular speed as it can be seen on figure 2.1. The center point of the vials is point O_1 and they spin around their axis with a ω_v angular speed, reverse to the ω_p spin. In the following mathematical equation, the „absolute" and the „relative" expressions refer to the parameters that were determined based on the XOY absolute and xO_1y relative coordinate systems. From this the motion of the ball with m_b mass next to the milling vial is the following.
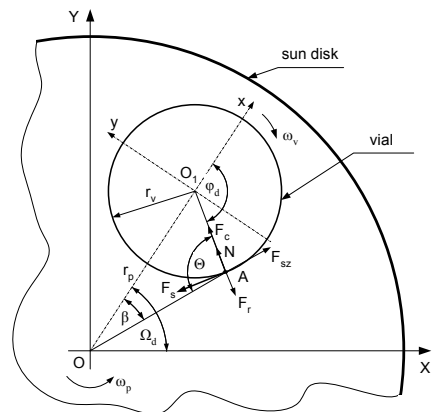

Figure 2.1. Force and motion conditions in a planetary ball mill

The forces that affect to the ball in a the milling vial are the delivering force and the relative force that affect from the center point of the sun disk and the vial, marked as F_{sz} and F_r. The N and F_s are normal and frictional forces, that arise from the interaction of the ball and the vial, and from the Coriolis effect the F_c force, and gravity. Using the D'Alembert principle the balls can be defined with static equilibratory equations if we take the accelerations as inercia forces, that are equal the multiplication of the mass and the acceleration of the ball. From this, the delivering force from the point O, the relative force from point O_1 and the Coriolis-force that affects towards O_1 the following can be written.

Based on Figure 2.1. the resultant of the forces in the system:

$$\Sigma \vec{F} = m_b \cdot (\vec{a}_{sz} + \vec{a}_r + \vec{a}_c) \tag{2.1}$$

$$N = F_r - F_c - F_{sz} \cdot \cos(\pi - \theta) \tag{2.2}$$

where *N* is the normal force that affects to the surface of the vial, that pushes the ball to the wall of the vial.

Determining the detachment angle

I assume that when *N=0*, then the ball disjuncts from the surface of the wall by itself. This critical criterion can be written as:

$$m_b \cdot \omega_p^2 \cdot \frac{r_p + r_v \cdot \cos\varphi_d}{\cos\beta} \cdot \cos(\pi - \theta) + 2 \cdot m_b \cdot r_v \cdot \omega_p \cdot \omega_v = m_b \cdot r_v \cdot \omega_v^2 \tag{2.3}$$

where φ_d is the angle of the ball disjuncting from the wall of the vial (Figure 2.1.).

Let the ratio between the vial angular speed and the sun disk angular speed be (ratio):

$$i = \frac{\omega_v}{\omega_p} . \tag{2.4}$$

After ordering and conversion the (2.3) equation, and by using the (2.4) equation, the angle of the ball disjuncting from the wall can be determined (Lü and Lai 1998). If the sun disk and the vial rotate in the opposite direction, the detachment angle will be the following:

$$\varphi_d = \arccos\left(-\frac{r_v \cdot (1-i)^2}{r_p}\right) \tag{2.5}$$

The effect of the ratio (i) to the detachment angle and the flight path of the ball

The detachment and influencing positions depend on the size of the vial (r_v), the position of the vial on the sun disk (r_p), and the ratio of the rotational speeds (*i*). When r_v and r_p are fixed, the detachment only depends on *i*, so it seems to be useful to determine those ratio values that make the ball go on different flight paths.

To determine the limit values of the ratio, I started from the equation 2.5. The limit values of the ratio in case of fixed geometrical parameters (r_p, r_v), omitting the deduction is the following:

$$i_{limit} = 1 - \sqrt{\frac{r_p}{r_v}} \le i \le 1 + \sqrt{\frac{r_p}{r_v}} = i_{kritikus} \tag{2.6}$$

From the (2.4) and (2.6) equations it can be stated that in case of a mill with given construction (r_p) and given milling vial (r_v) the rotational speed of the sun disk (ω_p) and vials (ω_v) must be set to reach the best milling output as the (2.6) equation to be true, because this is when the milling ball disjuncts from the wall. If the following condition is realized $i_{limit} \le i \le i_{kritikus}$, then the milling occures according to the effecting and friction method, when the kinetic energy from the milling balls to the powder is the largest.

In impact and friction mode (when $i_{limit} \leq i \leq i_{kritikus}$) the flight path of the ball can be easily determined by the basic principles of dynamics, as it can be seen on Figure 2.2. The energy in the moment of the effect can be divided into two components. Namely the normal component that causes the increase of the effective impact energy that reach the dust particles and the tangent component that can appear as friction energy.
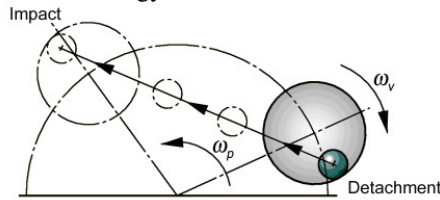

Figure 2.2. Movement of the ball after the detachment, when $i_{limit} \leq i \leq i_{kritikus}$

Determining the detachment speed (v_d)

For determining the energy released after the detachment of the ball, during the impact, it is essential to know the the speed and the direction of the ball at the point of the detachment. After determining the angle of the detachment (2.5.), the absolute point of detachment '*A*' (2.1. ábra) and the speed of the detachment can be calculated, assuming that the ball and the vial moves together in the moment of the detachment. The detachment speed in point '*A*' is the addition of the circumferential speeds of the sun disk and the vial.

2.1.2. The kinetic energy of the milling ball at the moment of the impact

From this point of the modelling (including the detachment speed determined above) I have built the model with my own algorithm. In the known and accessible literature sources I could not follow up the work of others, because:
  ➢ they don't show the calculations of the determination of the impact point, despite this is the most difficult and significant step of the model,
  ➢ they discard the size of the ball in the models of planetary ball mills, they consider it as a point. I can't find this simplification acceptable. On Figure 2.3. it can be seen that the φ_c angle that belongs to the actual impact point (*B*) can be several times higher than the value that would be in case of a ball considered as a point (point *B*', angle φ_c').

So with the model that I have set up I want to determine the exact place of the impact, considering the dimension of the balls. This way the influence energy can be determined more precisely.
To determine the real kinetic energy of the ball, the absolute speed of the impact point must be known. The actual impact speed is the difference between the calculated speed in the impact point and the detachment speed. We have to consider the radial component of this speed on the vial as the speed component that is needed for the determination of the kinetic energy.
As the ball disjoins from the wall of the vial, I assume that it moves with a constant linear speed of the detachment. The acceleration due to gravity is perpendicular to the tested surface of movement. In this case the ball's speed is only affected by the resistance of medium, but I discard this effect. I apply the kinetics of rigid bodies to write down the free movement of the ball, until it doesn't reach the vial again. The figure 2.3. shows the movement of the ball from the detachment until the influence, where points '*A*' and '*B*' mark the places of the detachment and impact.
It is essential to know the exact place of the point of the detachment, that is point '*B*', to determine the absolute speeds there. For this, it is important to know that in case of the rotational speeds of the fixed sun disk (ω_p) – and the vial (ω_v) and the already known detachment speed what is the angle of the vial (Ω_c) and to the vial what angle is it (φ_c) when the ball impacts.

I have determined the absolute speed of the impact point indirectly. The summerized calculus is the following.
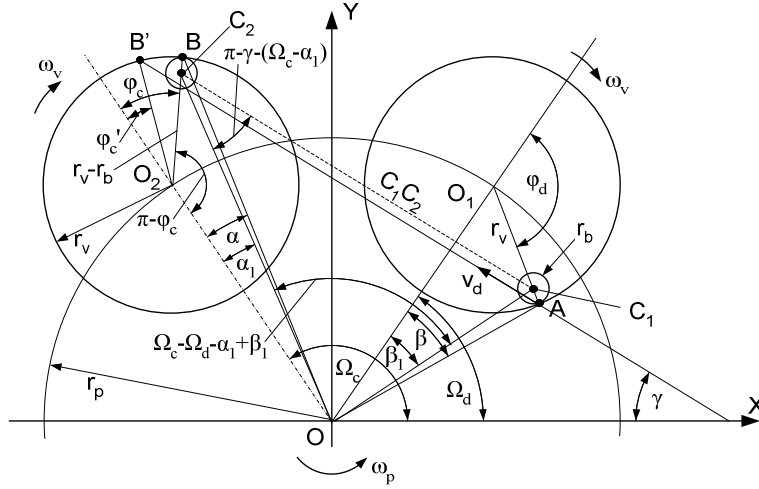

Figure 2.3. The movement of the ball from detachment to the impact and the geometry of the ball impact

Determining the parameters of the impact point with gradient method

For the determination of the impact point, I departed from the principles of the movement of the ball and the vial and from the geometrical characteristics of the structure. See Figure 2.3. that shows the geometrical relations of the ball impact. It is true to the relation between the movement of the ball and the vial from the aspest of the impact point that during the time while the ball gets to the impact point with detachment speed (v_d) starting from the moment of detachment, the vial at the same time does Ω_c-Ω_d angular rotation with ω_p angular speed around point 'O'. It's formula:

$$\frac{\overline{C_1 C_2}}{v_d} = \frac{\Omega_c - \Omega_d}{\omega_p} \tag{2.7}$$

Because of that the $C_1 C_2$ distance and the Ω_c angle is unknown, furthermore it is necessary to know the a φ_c angle, more relations must be found. According to figure 2.3. the geometrical relations for the $OC_2 O_2$ triangle are the followings:

$$\frac{\sin\alpha_1}{\sin(\varphi_c - \alpha_1)} = \frac{r_v - r_b}{r_p} \tag{2.8}$$

$$\overline{OC_2}^2 = r_p^2 + (r_v - r_b)^2 - 2 \cdot r_p \cdot (r_v - r_b) \cdot \cos(\pi - \varphi_c) \tag{2.9}$$

Also from figure 2.3. for the $OC_1 C_2$ triangle the followings are true:

$$\frac{\sin(\pi - \gamma - (\Omega_c \pm \alpha_1))}{\sin(\Omega_c - \Omega_d \pm \alpha_1 + \beta_1)} = \frac{\overline{OC_1}}{\overline{C_1 C_2}} \tag{2.10}$$

$$\overline{C_1 C_2}^2 = \overline{OC_1}^2 + \overline{OC_2}^2 - 2 \cdot \overline{OC_1} \cdot \overline{OC_2} \cdot \cos(\Omega_c - \Omega_d \pm \alpha_1 + \beta_1) \tag{2.11}$$

Despite of it is about basic mathematical and physical correlations, the equations (2.7-2.11) form a non linear equation system with five unknown quantities, in which the unknown parameters are the impact angle (φ_c), the angle of the vial in the moment of the impact (Ω_c), the distance between the center point of the ball and the rotational axis of the sun disk (OC_2) and the detachment point ($C_1 C_2$), and the angle (α_1) between OC_2 and OO_2. The determination of the 'φ_c' and 'Ω_c' parameters

is directly needed, the rest of the above mentioned parameters are only indirectly needed for the calculation of the absolute speed of the impact point. The problem is more difficult, because the impact point can be eather on the left or the right side of OO_2 (± $α_1$). During the solution it needs further attention that the variables in the different phases of the movement can take values in different intervals.

I have solved the previous equation system numerically, with the so-called gradient method. I have done the caldulations within definite limit values, determined with construction. For the constructions I used Pro/ENGINEER software package.

Determination of the speed of the impact point (v_b)

After determining the place of the impact ($Ω_c$) and angle ($φ_c$) above, the absolute speed of the point can be calculated in the impact point 'B'. The speed of the impact in point 'B' is the addition of the peripheral speed of the sun disk and the vial. The components of the absolute influence speed comes from the difference of the corresponding components of the detachment speed and the impact point speed.

The determination of the impact energy (E_b) and the output of the milling (P)

For the determination of the kinetic energy of the ball, that is the impact energy, the normal direction components of the absolute impact speed. The angle where the impact of the ball happens to the wall of the vial ($φ_c$), determines the amount of energy that is delivered from the ball to the dust particles. The effective impact speed (v_{in}), that indicates the impact energy is the normal direction component dissociated to the direction of radiation of the milling vial.

After determining the values mentioned above, the calculation of the effective impact energy that is liberated at one collision during the mechanical milling process is the following:

$$E_b = \frac{1}{2} \cdot m_b \cdot v_{in}^2 \qquad \text{[J/impact]} \qquad\qquad (2.12)$$

The tangent direction component (v_{it}) gives the increase of the kinetic energy (E_s) that is also formed during the milling process.

$$E_s = \frac{1}{2} \cdot m_b \cdot v_{it}^2 \qquad \text{[J/impact]} \qquad\qquad (2.13)$$

The energies that can be determined from the equations (2.12) and (2.13) transferred from the milling ball to the dust particles as many times as the balls collide with the wall of the vial. The impact frequency, that is the number of the collisions of the ball to the wall of the vial per second can be determined as the following:

$$f_b = \frac{1}{T_1 + T_2} \qquad \text{[s}^{-1}\text{]} \qquad\qquad (2.14)$$

where T_1: is the time, while the ball gets from the first detachment point to the first impact point,
T_2: is the time, that elapses after the first impact, until the second detachment.

But in practice, the milling is not applied with one ball, so the effective impact frequency f_{eff} can be determined, considering the number of balls in the vial:

$$f_{eff} = f_b \cdot N_b \qquad \text{[s}^{-1}\text{]} \qquad\qquad (2.15)$$

where N_b: is the number of the balls in the vial.

Knowing the energy liberated during the impact (E_b) and the effective impact frequency (f_{eff}), the output of the milling process (P) is:

$$P = f_{eff} \cdot E_b \qquad [W] \qquad\qquad (2.16)$$

The output exposited above is capable for the comparison of the millings with different impact energies. The bigger output delivered from the balls to the particles means that shorter time is needed for the milling process.

Considering that the millings are done for a definite time (t) with definite amount of powder (m_p) measured into the milling vial, the cumulative energy (E_{kum}), normalized to the quantity of the milled material can be determined that is carried in during the milling:

$$E_{kum} = \frac{E_b \cdot f_{eff} \cdot t}{m_p} \qquad [J/g, \ Wh/g] \qquad\qquad (2.17)$$

Based on the calculation method showed in this chapter the impact energy and impact frequency of the ball can be determined and it can be seen that they can be individually adjusted, if the parameters of the milling are set correctly. By changing the number of the balls, the impact frequency (f_{eff}) of the ball can be adjusted, while the impact energy of the ball (E_b) stays the same. On the other hand, by changing the diameter and density of the ball, the ball impact energy can be changed without the change of the impact frequency. It is important to note that the showed model is true and valid if the following is true to the ratio (i) of the speeds of the sun disk and the milling vial $i_{limit} \leq i \leq i_{kritikus}$.

2.2. Experiment devices and methods of the production of Ba-hexaferrite

2.2.1. The places of the experiments

The experiments and the measurement that were needed to reach the aims listed in Chapter 1. were executed in many scenes, in several research institutes and industrial companies. Most of them were made by me and a few were made with the help of other researchers.

The milling experiments were done in the Bay Zoltán Foundation, Institute of Materials Science and Technology (BAYATI), while the conditions of the research were present there. I also did the production of Ba-hexaferrite basic material by high energy milling here. The next technological step of the ferrite production is the pre-sintering of the milled powder. Initially this operation was made at TKI-Ferrit Kft. (Budapest). Later we had the chance to purchase a new tube furnace in BAYATI, that is able to heat up to 1500 ^{o}C in vacuum or even in inert gas medium. From this point I could do the pre-sintering too in BAYATI. Following the technological line of the hexaferrite, the moulding and the finishing sintering were made at the site of TKI-Ferrit by the employees of TKI.

The examination of the structure (XRD) and morphology (SEM, TEM) of the produced grinds and prepared samples were made with the help of the associates of the Chemical Research Center of the Hungarian Academy of Sciences (MTA-KKKI).

The classification of the magnetic characteristics of the produced Ba-hexaferrite bulk material took place at the Research Institute for Solid State Physics and Optics of the Hungarian Academy of Sciences (MTA-SZFKI), the determination of the microwave parameters were done at the Budapest University of Technology and Economics Department of Broadband Infocommunications and Electromagnetic Theory (BME).

From the above written things it can be seen that I had to build relation to several notable research institutes that was very time-consuming, but it gave a remarkable help for finish my work with success.

2.2.2. Introduction of the experimental devices

The measurement of the basic materials, sampling

I have measured the materials used for the experiments with an „EXPLORER" type digital laboratory balance. The accuracy of the balance was 0,001 g. The use of protective devices is

compulsory during the preparation of the materials. Because of this I was wearing rubber gloves, dust protection mask and protective glasses in all cases.

For the milling and material examinations I took the required amount from the basic materials with the common method of chemical analitics.

Device used during the millings

The milling experiments were executed with a German Fritsch „pulverisette 4" Vario-Planetary Mill type planetary ball mill (Figure 2.4.).
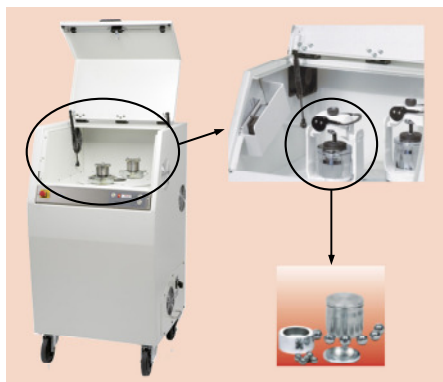

Figure 2.4. Fritsch Vario-Planetary Ball Mill „Pulverisette 4" planetary ball mill

This type of mill makes possible a higher energy milling, compared to the former, similar mills (because of the wide range of selection of the milling parameters). The device is ideal for mechanical activating and alloying of different materials. The main field of it's use is material research.

The active capacity of the mill is 2x30 ml in case of using 80 ml milling vials. The device made it possible for me to choose the ideal milling vial and ball material, size and amount for the material to be grinded and furthermore it let me to adjust the parameters that affects the milling process precisely.

Tube furnace applied at the pre-sintering

For the pre-sintering operation I have done a K-1550 ºC Vacuum/Argon type tube furnace was used with 1500 W electrical output. The nominal heating temperature of the furnace was maximum 1550 ºC. The active size inside the furnace was Ø65x150 mm. The accuracy of the set temperature in the middle was ±0,5% at steady-state. The free controlling of the furnace is with a PID controller with digital display. This HAGA KD48P type controlling unit operates and controls the temperature, the heat up speed, the gas load and the vacuuming too.

2.2.3. Basic and additional materials used during the experiment

The chemical composition of the required W-type Ba-hexaferrite can be described with the following formula: $Ba(Zn_{0.5}Ni_{0.5})_2Fe_{16}O_{27}$. I have produced the samples with this composition starting from $BaCO_3$ (Reanal) and ZnO (Reanal) and $NiCO_3$ (Riedel) and Fe_2O_3 (Bayferrox) basic materials. These materials are qualificated and are commercially available.

I call auxiliaries the additional materials applied during the milling, that were mostly applied to reach advantageous milling conditions. These were the distilled water, acetone, ethanol and oleic acid.

2.2.4. Milling experiments

I have approached the experimental production of nanocrystal hexaferrites by high energy milling from several directions. I have examined the effects of milling and the material to each other in all of the cases. First I have examined if there is any solid-state reaction in the basic materials during milling. In the second part I started the production of W-type Ba-hexaferrite from the full composition, homogenized and milled basic materials, followed the whole technological line (pre-sintering, milling, moulding, final sintering). In the third part I have examined the effect of different milling media (air, distilled water, ethanol, acetone, oleic acid) to the milling set and the formed grain size. In the followings I show this three examination part, but before that it is important to clear that how and what aspects I chose from the different technological parameters of the milling.

The parameters of the milling experiments

The most important parameters that affects the milling process can be seen on Figure 2.5.
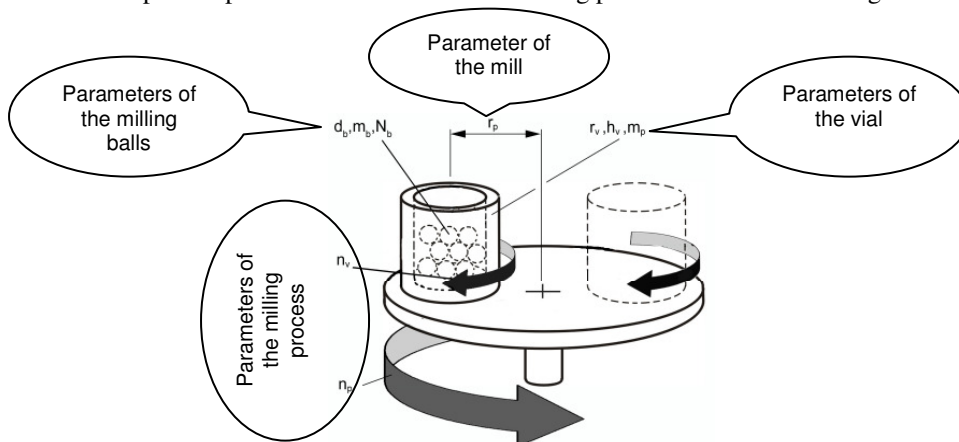

Figure 2.5. Parameters that affects the milling process in a planetary ball mill

Before the start of the milling experiments, I have considered all of the parameters and condition that take part in the tests. I have written an inspection record of every milling operation. I have recorded every important experimental condition, adjusted parameter, milled material and milling aids, sample identification, etc. in the inspection record, for the latter easy reconstruction of the experiments if needed.

The milling parameters to be determined were the following:

> ➢ speed of the sun disk (n_p)
> ➢ ratio between the sun disk and the vials (i)
> ➢ determining the milling cycle (duration of milling and stop within a cycle)
> ➢ determinating the duration of the milling

I have executed the millings with stainless steel milling set, where the volume of the vial was 2x80 ml, the diameter of the balls was 10 mm. In my experiments, the amount of the weighed portion of the powder was m_p=20 g, and I applied 25 pieces of milling balls and the mass ratio of the powder and the balls was 1:5, considering the fact that I used 80 ml vials. I have determined the speed of the sun disk and the ratio according to the results of the theoretical calculations, written in chapter 2.1. in a way the settings to be optimal from the side of the impact energy and output of the ball too. For this I have determined the sun disk speed to be n_p=400 rpm and the ratio to be i=2,25. The precise adjusting of the milling parameters and the controlling of the mill is ensured by the software that is provided by the manufacturer of the mill. The software has graphical user interface, so the required parameters for the milling process can be set and saved easily and quickly.

The milling of the basic materials added in different order

In the first phase of the experimental work I have put the basic materials in different order and at different times in the vial to inspect the effect of the basic materials to each other.

For the production of the W-type Ba-hexaferrite material that's formula is $Ba(Ni_{0,5}Zn_{0,5})_2Fe_{16}O_{27}$ I have measured the following amounts from the basic materials, keeping to the rules of stochiometrics:

Table 2.1. The measured amounts of the basic materials

Raw material	Fe_2O_3	ZnO	$NiCO_3$	$BaCO_3$
Manufacturer	Bayferrox	Reanal	Riedel	Reanal
Molecular mass [g]	159,6922	81,3894	118,7026	197,3362
Required amount for production 100g hexaferrite [g]	76,272	4,859	7,087	11,782

For the easy comparability I have kept the milling parameters at the same level at all of the variations. I have examined the produced materials after the pre millings and the final millings by XRD, SEM and TG/DTA methods. I have applied the millings in the variations that can be seen in table 2.2.

Table 2.2. Milling variations to the milling of the basic materials

Variation		Basic material			
Sample No.	Method of milling	Fe_2O_3	ZnO	$NiCO_3$	$BaCO_3$
1.	premilling for 4 hours	+	+	-	-
	further milling together for another 4 hours	+	+	-	+
2.	premilling for 4 hours	+	-	+	-
	further milling together for another 4 hours	+	-	+	+
3.	premilling for 4 hours	+	+	+	-
	further milling together for another 4 hours	+	+	+	+
4.	homogenizing* for 0,5 hours	+	+	+	+
5.	milling for 8 hours	+	+	+	+
6.	premilling for 4 hours	-	+	+	+
	further milling together for another 4 hours	+	+	+	+
7.	premilling for 4 hours	-	-	+	+
	further milling together for another 4 hours	+	+	+	+
8.	premilling for 4 hours	-	+	-	+
	further milling together for another 4 hours	+	+	+	+

* Homogenizing means a type of milling when the parameters are chosen in a way that the mill only mixes the material

+ the material is present at the milling process

- the material is not present at the milling process

The production of W-type Ba-hexaferrite by the homogenizing and high energy milling of all the components at the same time

In case of two composition variation (see Table 2.2., 4. and 5.) I have executed the whole technological line. In case of the variation 4. by modelling the conventional ceramic technology I have produced the W-type hexaferrite with low energy milling („homogenization"). The variation 5. was an experimental high energy milling to produce W-hexaferrite. The steps of the technological line of the sample variations 4. and 5. can be seen on Figure 2.6.

By following this technological line I could produce W-type Ba-hexaferrite. The characteristics of the produced material are written in chapter 3.2.2.
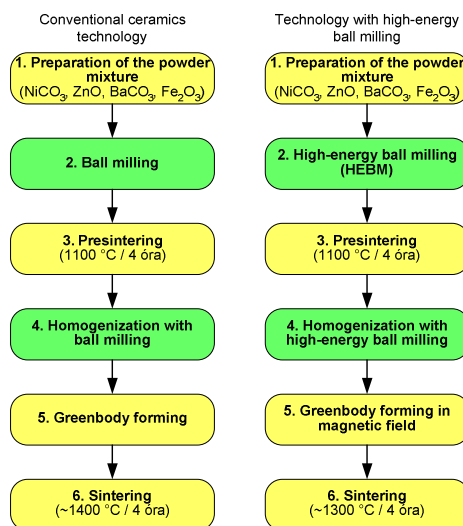

Figure 2.6. The steps of the conventional (left) and the new (right) technology

Milling experiments in different media

In this experimental part I write down the experiences of milling the basic materials with different moistening media and additives. In the choosing of the the media, the industrial experiences and the professional literature helped me. I applied every milling on full basic material composition (variation 5., see Table 2.2.) samples, in the following media:

➢ ethanol (25 ml)
➢ acetone (25 ml)
➢ distilled water (25 ml)
➢ oleic acid (additive) (0,045 ml that is 0,2 mass percent)

The preliminary aim of the milling experiments in different media was to improve the conditions (agglomeration, adhering powder on the milling set) of the dry milling (only in air medium).

2.2.5. Methods of examination of materials applied to the checking and featuring of the samples

During the experiments, the structure of the produced samples were analyzed with X-ray diffraction (XRD), the morphology with Scanning Electron Microscope (SEM) and with Transmission Electron Microscope (TEM) tests. I tried to follow the formation of the hexaferrite and the M → W-type changing process with thermal gravimetric analysis. At the end of the

technological line, the measurments of the magnetic characteristics of the W-type Ba-hexaferrite samples were done with a Foner-type vibrating sample magnetometer (VSM). At the end, the microwave measurements were done with the devices that were developed at the Department of Broadband Infocommunications and Electromagnetic Theory of Budapest University of Technology and Economics (BME).

The X-ray diffraction examination of my tests were done by István Sajó (MTA-KKKI) with a Philips PW 105 goniometer, using CuK_α radiation, the parameters were 40 kV, 35 mA, graphite monochromator, proportional counter. The average crystallite size were determined by Scherrer-method. The given result for the crystallite size of the material is representative for the average size of the coherent scattering ranges. This data does not makes a difference between the size of the grains that are separated with big angle grain boundary and the size of the grains that exist individually.

With the Scanning Electron Microscope shots I have mostly examined the effects of the milling and sintering to trace the morphologic change of the samples. From the pictures I got precise information of the shape of the grains and the approximate size of them can also be estimated. The pictures from my samples were made by Dr. Katalin Papp (MTA-KKKI), with a Hitachi S-570 type microscope.

With the transmissional electronmicroscopic examinations I wanted to know more about the morphological characteristics of the formed grains. The shots were made by Rózsa Takács (BAYATI) and Péter Németh (MTA-KKKI) with a Jeol 200A and a MORGAGNI 268D type device.

During my research the thermal gravimetric analysis were made by László Trif in BAYATI with a Setaram Setsys 16/18 type device. For the measurements he used synthetic air (80% N_2, 20% O_2) medium, between 20-1500 ^{o}C temperature range, with 10 K/min heat up speed, using 100μl Al_2O_3 vials.

In the Mössbauer spectroscopic measurements, Zoltán Németh (ELTE) helped me. With the measurements my aim was to prove the presence of the W-type hexaferrite phase in the material produced in the milling experiments.

The measurement of the magnetic characteristics (magnetic saturation, coercive force) of my produced samples were made by Dr. László Kiss (MTA-SZFKI) and Sándor Hosszú (BME) with a vibrating sample magnetometer. According to the guidance of László Kiss I could do several measurements by myself on my own samples.

3. RESULTS

3.1. The application of the model set up to the planetary ball mill and results of calculations

With the calculation method that was introduced in chapters 2.1.1. and 2.1.2. I have determined the milling energies of the FRITSCH P4 type planetary ball mill that was applied during the measurements, in case of differend setting parameters. During the calculations I considered different sun disk speeds and ratio to examine the whole speed range of the mill and the path of motion of the balls to fulfill the influence and friction method, that $i_{limit} \leq i \leq i_{kritikus}$ to be true. I have done the calculations to i = 1; 1,5; 2; 2,5; 2,96 values.

In the first part of the calculations, when determining the detachment angle and speed I experienced in case of the geometrical relation (r_p, r_v, r_b) and ratio (*i*), that equal detachment angles belong to the increasing sun disk speed, while the value of the detachment speed increases by direct correlation to the speed of the sun disk.

After the determination of the impact angle and speed, I have rated the theoretical impact energies to different sun disk speeds, in case of one ball. The curves that were designed from the results of the calculations can be seen on Figure 3.1.
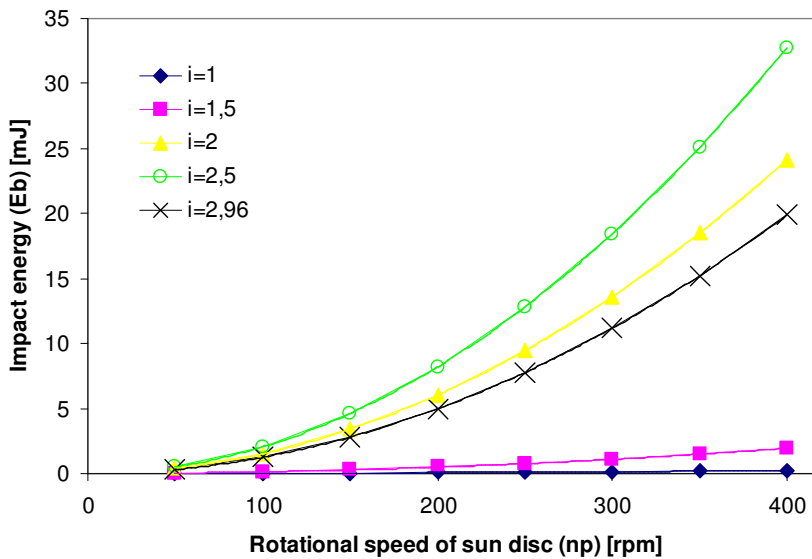

Figure 3.1. The change of the impact energy (E_b) in the function ($E_b(n_p)$) of the sun disk rotational speed (n_p) and the ratio (i)

It can be seen from Figure 3.1., that increasing the speed of the sun disk increases the impact energy by second power until reaching a certain ratio. It can be seen that at speed ratio *i=2,96* the curve of the impact energy is between the *i=1,5* and *i=2* curves. From this it is possible that there is an optimum between the *i=2* and *i=2,96* values, where the impact energy is the highest.

This assumption is proved by the group of curves showed on Figure 3.2. The curves show the changing of the impact energy by the increasement of the ratio, belonging to different sun disk speeds. From the diagram it can be detected that in case of the given geometrical relations and the set parameters, the highest impact energy can be reached at somewhere *i=2,5*. If the impact frequency of the balls is also considered, that is mainly in the function of disjuncton and impact angles, than the output of the milling process can be determined by using the (2.16) correlation.
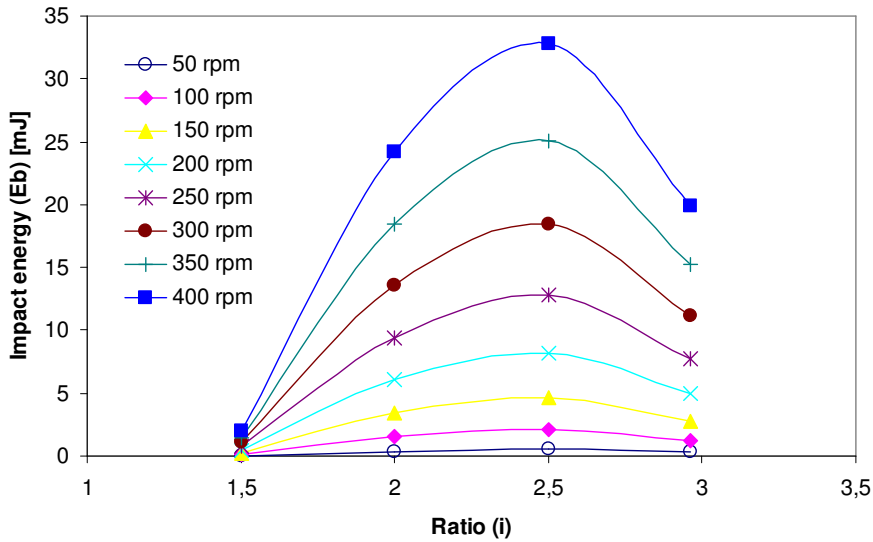
Figure 3.2. The changing of the impact energy (E_b) in the function ($E_b(i)$) of the increasement of the ratio (i) at different rotational speeds values (n_p)

If we study the theoretical outputs that belong to different sun disk speeds and speed ratio (Figure 3.3.), we can see that higher and higher output values belong to the increasing speeds. The calculated curves are cubic.
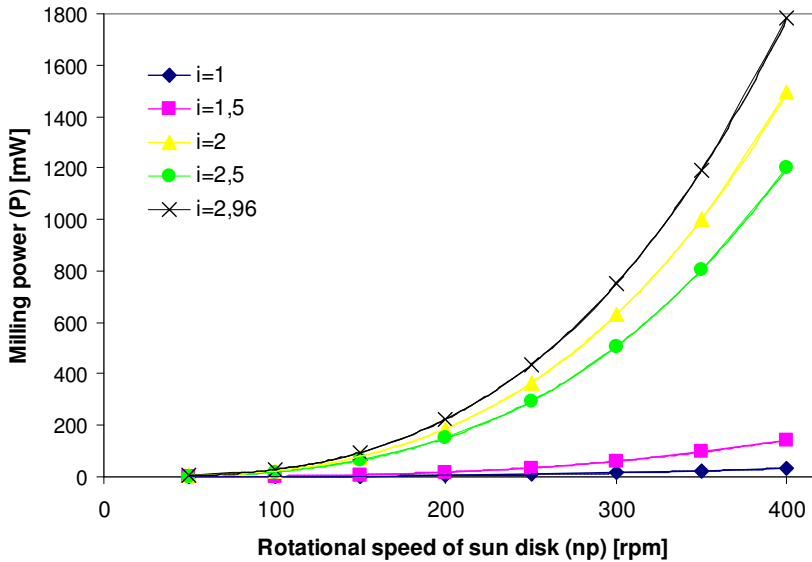

Figure 3.3. The changing of the milling power (P) in the function ($P(n_p)$) of the sun disk rotational speed (n_p) and the ratio (i)

In the contrary of the changing of the impact energy showed on Figure 3.1., on Figure 3.3. it can be seen that the values that belong to the curves *i=2,5* are lower than *i=2* and *i=2,96*. The result is surprising because a lower output belongs to the speed ratio that results the highest impact energy. This can be explained with the lower impact energy at this ratio (*i=2,5*), which means that the balls spend more time on the wall of the vial.

If I draw the milling output (power) in the function of the ratio at different sun disk speeds (Figure 3.4.), than the optimal speed ratio from the aspect of the milling output can be determined. On Figure 3.4. it is about $i=2,96$ value.
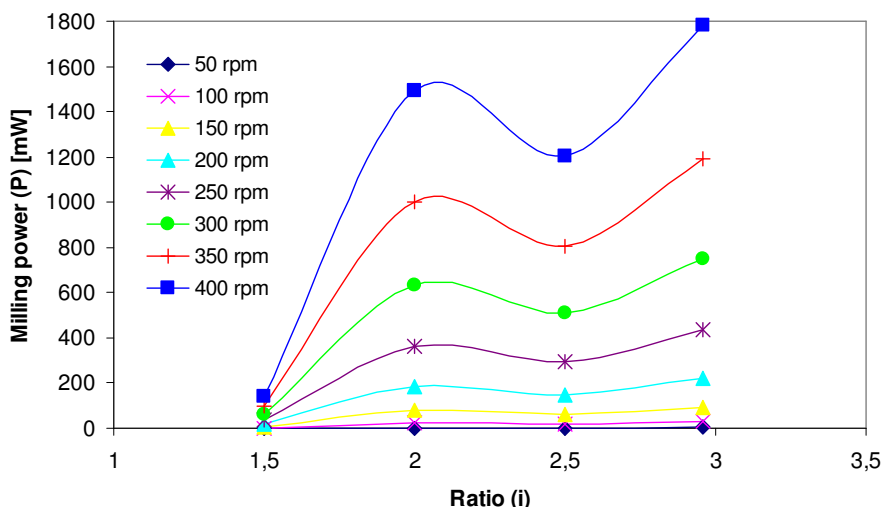

Figure 3.4. The changing of the milling power (P) in the function (P(i)) of the increasement of the ratio (i) at different sun disk rotational speed values (n_p)

With the help of the Figures 3.2. and 3.4. an optimal ratio range can be defined that is maximal from the aspect of impact energy and milling output too. This range is obviously $i=2\text{-}2,5$, besides the determined parameters.

According to the correlation (2.17) that belonged to the amount of the milled powder, we can see the changing of the total energy input during the milling in the function of the sun disk speed (figure 3.5.) and the ratio (3.6. figure) at different ratios and sun disk speeds. The diagrams and the figures showed above (Figures 3.3. and 3.4.) are totally the same in their character, while the marked total milling energy values are calculated based on the amount of the actually milled powder.
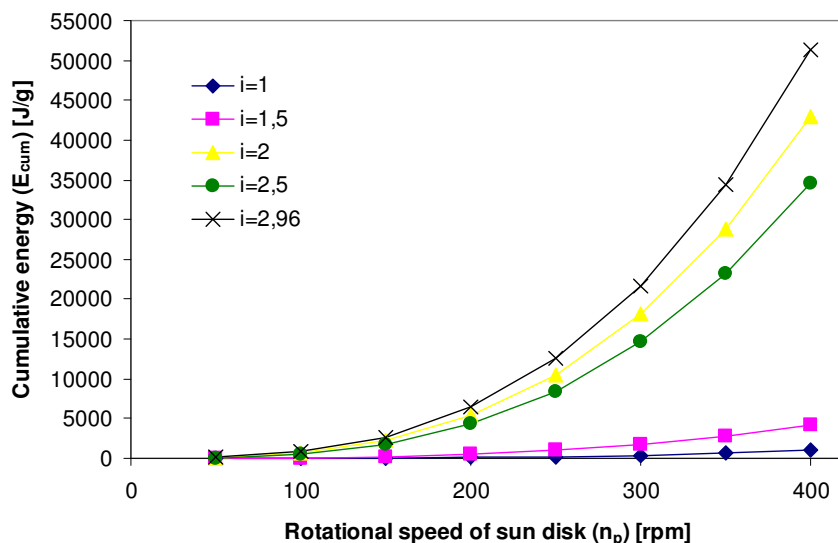

Figure 3.5. The changing of the cumulative energy (E_{cum}) during the milling, referenced to mass in the function ($E_{cum}(n_p)$) of the sun disk rotational speed (n_p) and the ratio (i)
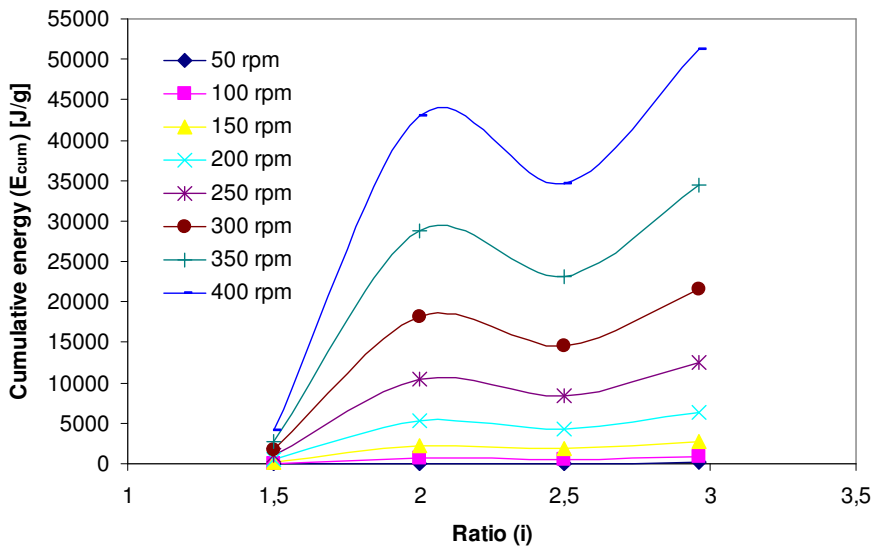
Figure 3.6. The changing of the cumulative energy (E_{cum}) during the milling, referenced to mass in the function ($E_{cum}(i)$) of the increasement of the ratio (i) at different sun disk rotational speed values (n_p)

Although I have determined the results (diagrams) of the calculations of my model to given starting parameters, showing the adaptability of the method, but it is capable of the description of any chosen milling processes with other settings and geometrical parameters in case of a planetary ball mill.

The effect of the change of the size of the milling ball and milling vial and the number of balls

I have determined the above mentioned results in case of fixed ball and vial sizes. I have made further calculations to examine the effect of change of the size of the milling set (ball, vial) on the impact energy and output.

First I have examined only the size change of the vial with the same ball size then I have increased the ball size and kept the vial size. Finally I have doubled the ball size and the vial size too. I have compared the results to the results that belong to the setting parameters of n_p=400 rpm and i=2. The diagram that shows the changing of the impact energy can be seen on Figure 3.7.

It can be clearly seen that the results of the calculations bring the hoped increasement of the impact energy. From the results we can accept that the increasement of the size of the vial does not effect the increasement of the impact energy as the changing of the ball size. The joint changing of the size of the milling set (ball, vial) leads to the highest impact energy.

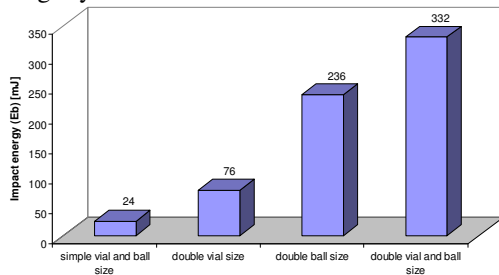A slightly less increasement was detected in the change of the milling output (Figure 3.8.).

Figure 3.7. The impact energy during the changing of the size of the milling ball and vial
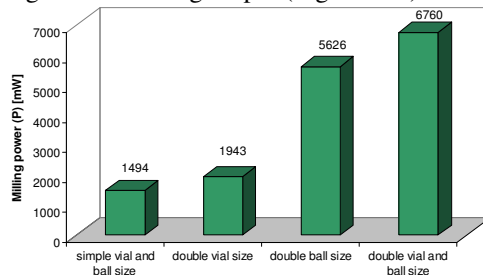

Figure 3.8. The milling power during the changing of the size of the milling ball and vial

From the calculated data and diagrams the optimal milling parameters can be picked that allow the effective work. Although the calculations were done and showed in case of the geometrical relations of a certain type of mill (Fritsch Pulverisette 4), the model can be applied to any kind of planetary ball mill by keeping the given boundary conditions.

In total to the effect of the size of the milling mill and vial to the impact energy and output it can be determined that if we have more milling sets, by using them further energies can be obtained from the planetary ball mill (besides the same main plate speed and ratio), increasing the effectiveness of the milling and decreasing the time.

Based on the results of the calculations and the nomograms (Figures 3.2. and 3.4.) the optimal setting of the mill can be determined, that lets the most effective work from the aspect of the milling job. During my researches I haven't found similar nomograms in the professional literature of modelling planetary ball mills. By using my method, for example in case of milling material with lower hardness, the smaller impact energy can also allow quick work, sparing the milling set and decreasing the load of the mill.

3.2. Results of experimental production of Ba-hexaferrite

3.2.1. Milling basic material added in different order

I have examined in a row the pre grinded and final materials showed in Table 2.2. with XRD, SEM and TG/DTA methods, and I summarize the results in the following.

According to the X-ray diffraction (XRD) I have reached less than 100 nm average crystallite size with all of the pre-milled and final samples. Examining the results of the x-ray tests it can be determined that only in case of one variation, the 2. showed formation of new phase ($NiFe_2O_4$) after the pre-milling (Figure 3.9.). During the other cases the x-ray structure test couldn't show the presence of new phases.
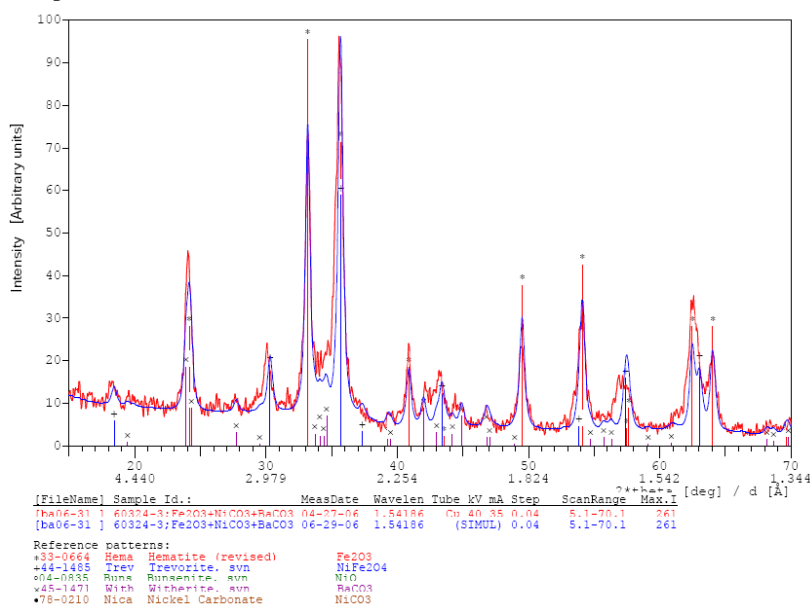
Figure 3.9. X-ray diffraction pattern of the sample 2.

According to the thermal gravimetric analysis, a few process were obviously identifiable (for example the outgoing of the bound water, decomposition of components), but the temperature of the ferrite formation could not be detected precisely. Only in case of the whole compositions (variations 4. and 5.) was observable a kind of phase transformation at about $1300^{o}C$ (Figure 3.10.). This probably means the ferrite formation, on the figure a black circle marks the place where I assume

the ferrite formation. According to the literature, the temperature range of the formation of ferrite is between 900 – 1450 °C depending on the production technology. The importance of the thermal gravimetric analysis was to determine the sintering temperature of the whole technological line starting from the above mentioned.
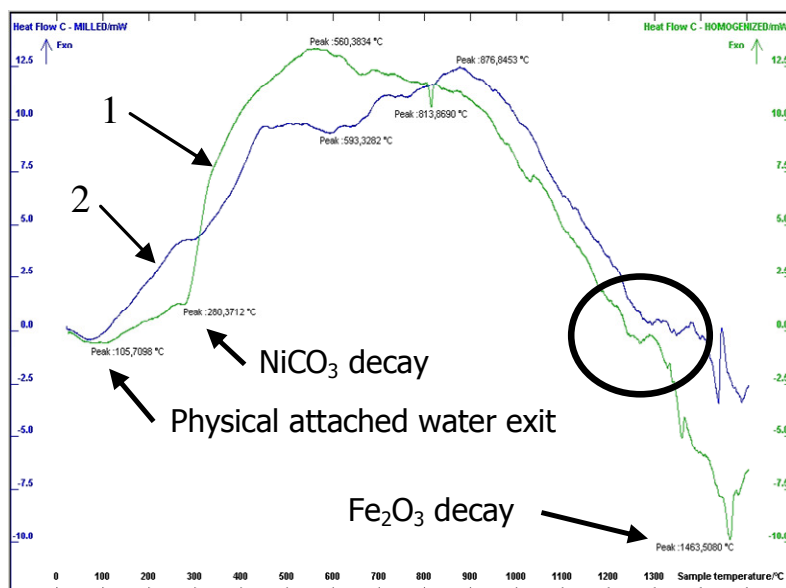

Figure 3.10. Comparison of the DTA curves of the samples that were produced by "homogenization" (variation 4. (**1**)) and high-energy mechanical milling(variation 5. (**2**))

At the end of the milling experiments when the components were added in different order at different times it could be determined that I have reached less than 100 nm average crystallite size by setting the milling parameters correctly and except for one case (Table 2.2., milling variation 2.) the milling did not result the formation of new phase. In case of one sample, the required higher reaction ability of the formed nano-grained (that means increased relative surface) could not be proven. I could also show that the formation of W-hexaferrite comes off in the presence of all of the components. Because of this in the following experiments of producing W-hexaferrite I only examined the milling of all of the components at one time together.

3.2.2. Producing W-type Ba-hexaferrite by homogenizing all of the components at the same time with high energy milling

I could produce W-type Ba-hexaferrite by following the steps of the technological line that were showed on figure 2.6., and according to the x-ray structure examination, in case of variation 4. (that followed the conventional technological line) the the phase purity of the material was 80% and in case of variation 5. the phase purity of the material was 90% (figures 3.11. and 3.12.). I have checked the formed structures and phases after each technological step by X-ray diffractional test.
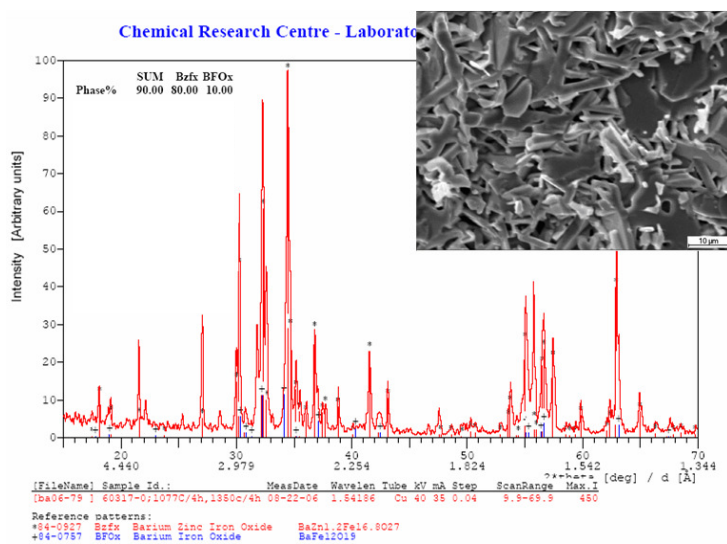
Figure 3.11. X-ray diffraction pattern and SEM micrograph of homogenised (variation 4.) W-type Ba-hexaferrite sample

On the diffractogram of figure 3.11. can be seen that besides 80 % W-phase, 10 % M-phase left, that did not transform. This can be explained with the larger average grain size and the lower reactivity that comes from it. Considering the morphology of the sample (figure 3.11. upper right corner) we can say that by following the conventional technology, the structure became lighter that consists of about 1 μm size grains.
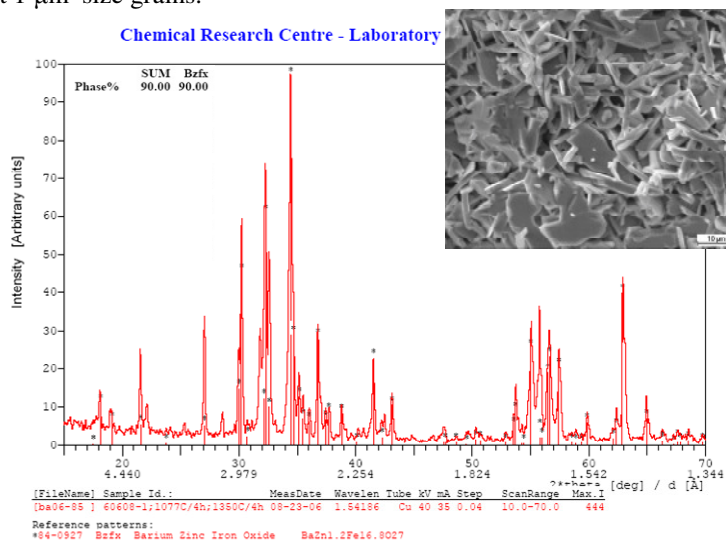
Figure 3.12. X-ray diffraction pattern and SEM micrograph of high-energy milled (variation 5.) W-type Ba-hexaferrite sample

The sample that was produced by high energy milling showed nearly clear phased material (figure 3.12.). Considering the morphology, compared to the material that was produced by homogenization, the porosity of the material from variation 5. was lower (although I haven't checked the porosity with pore size analysis) and the average crystallite size was also around 1 μm. According to the pictures of the SEM fracture test it can be seen that the n both cases the shape of the grains were hexagonal plates. For further examination I had the chance to use a Mössbauer-

spectrometer, that also confirmed the results of the X-ray analysis. During the two examinations I have used the russian H-6 W-type Ba-hexaferrite for calibration that is available and sold by the Ferrite Domen Co.

3.2.3. Milling experiments in different media

According to the results of the XRD analysis from the samples from millings in different media, I established that the millings in different media besides the same milling parameters result different crystallite size (Table 3.1.).

Table 3.1. Crystallite sizes reached with milling in different media [nm]

		starting sizes	after dry milling	Type of milling media or additive			
				etanol	dist. water	acetone	oleic acid
raw materials	Fe_2O_3	>1000	25	494	247	110	*29*
	ZnO	987	52	197	197	110	*34*
	$NiCO_3$	2,5	52	110	110	52	*25*
	$BaCO_3$	247	25	41	76	41	*25*

As it can be seen from the table, the oleic acid milling resulted the most close-grained structure. In this case the average grain sizes came by using the Scherrer equation as following: Fe_2O_3 = 29 nm; ZnO = 34 nm; $NiCO_3$ = 25 nm; $BaCO_3$ = 25 nm. From the diffractional spectra it can also be stated that during the milling with distilled water, Zn-OH formed that may be harmful during the further technological steps.

I have experienced significant differences between the millings applied with different media (distilled water, acetone, ethanol) or additive (oleic acid), and I got to the following statements:

➢ The applying of liquid media or appropriate additive during the millings eliminated the adherence of the grain to the wall of the vial and to the balls. This resulted better milling conditions.

➢ The abrasion of the milling set (vial, balls) remarkeably decreased.

➢ In case of the milling with oleic acid, the efficiency of the additive is significant, because even by using 0,2 mass percent – by making almost dry conditions – was very effective.

At the end of the former additive free milling experiments, the grain became heavily agglomerated and adhered to the surface of the vial and balls. This led to problems when emptying the mill and caused significant material loss too. In case of the millings with oleic acid, these problems totally disappeared. Another advanatage of using oleic acid compared to the millings with other liquids is that there is no need to dry the grain after milling, that means further spare in time and energy during the production. This fact can be prominent during the industrial adaptation, when producing materials in greater amounts.

In this phase of the experimental work I examined that how do the additives that are useful during the milling affect the further technological steps of the production and the formed phases. The results showed that in the samples that were produced with milling in organic materials (acetone, oleic acid) consisted the requested W-ferrite (Figure 3.13.) in a higher amount in pre-sintered state and in final state, than the samples that were produced with ethanol or water.
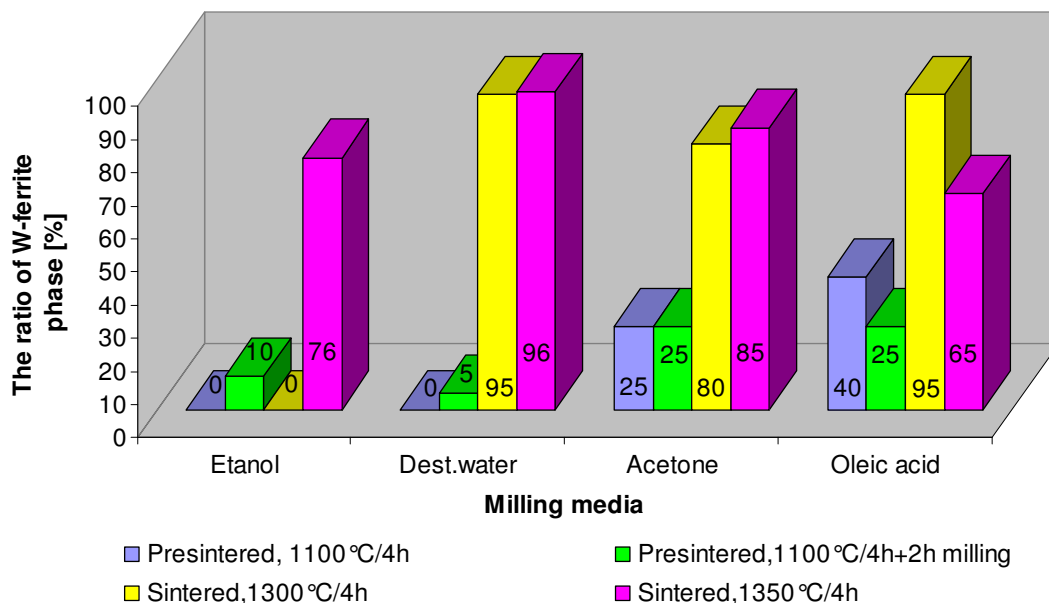
Figure 3.13. The ratio of W- ferrite phase after each technological step,
in case of different milling media

During the tests that were applied to eliminate the negative effects of the dry milling by using surface active materials and additives, I have determined the advantageous effects of the organic additive (oleic acid) that has no harmful effects on the further technological steps.

The results in the following chapter show the characteristics of the material that were produced by another full technological line. In these cases I did the millings adding oleic acid, because of it's advantageous properties, mentioned above.

3.2.4. The parameters of the end product, that is produced by milling

I have reproduced the W-type barium-hexaferrite by following the whole technological line (Figure 2.6.), but in this case I have used the mentioned oleic acid additive during the high energy milling.

The first technological step is high energy milling. During the milling I could reach an average crystallite size below 100 nm in case of all of the components (Fe_2O_3 35 nm, ZnO 23 nm, $NiCO_3$ 55 nm, $BaCO_3$ 21 nm). I have proved this by the results of the X-ray powder diffraction analysis.

The milling was followed by a pre-sintering, that was applied by TKI-Kft. The heat treatment was in a continuous chamber kiln, in ceramic boats at 1100 °C temperature for 4 hours in air. By the pre-sintering, new phases originated in the material, that was detected by X-ray tests. On figure 3.14. the XRD spectrum of the material can be seen. The material consisted of the following phases after the operation:

➤ 8% hematite (Fe_2O_3), average crystallite size: 494 nm

➤ 24% magnetite (Fe_3O_4), average crystallite size: 494 nm

➤ 65% M-type Ba-hexaferrite ($BaFe_{12}O_{19}$), average crystallite size: 247 nm

➤ 3% W-type Ba-hexaferrite ($BaNiZnFe_{16}O_{27}$), average crystallite size: 165 nm
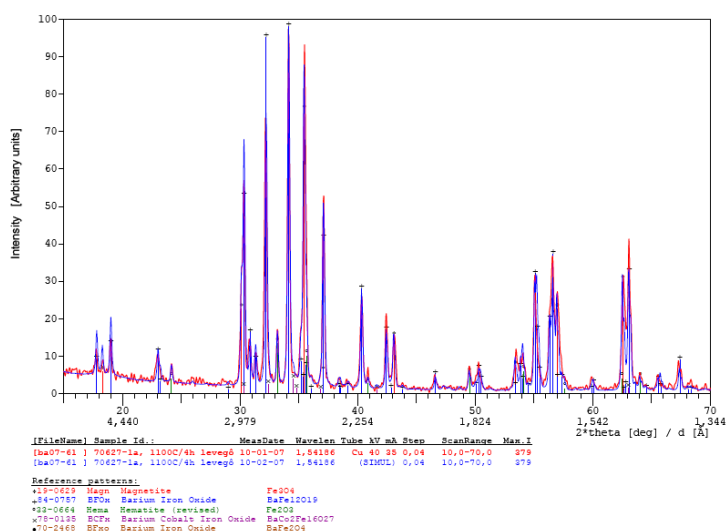
Figure 3.14. The X-ray diffraction pattern of the pre-sintered sample

The M-type Ba-hexaferrite was present in the greatest amount in the material and it was identified by High Resolution Transmission Electron Microscope (HRTEM) too. On figure 3.15. the picture of this can be seen.
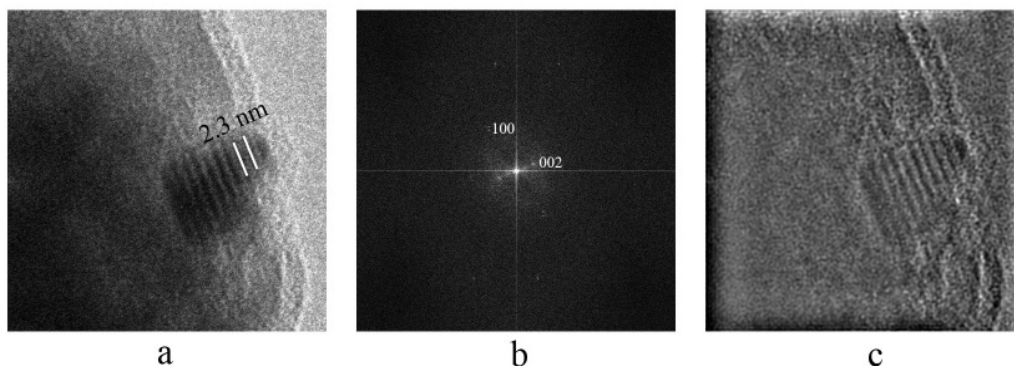

Figure 3.15. (a) HRTEM image of an M-ferrite grain along [010],
(b) Fast-Fourier transform calculated from (a), (c) background filtered image

The pre-sintering was followed by another high energy homogenizing milling. After the operation, the X-ray powder diffractional test did not show new phases compared to the per-sintered material, but the ratios and the average crystallite sizes slightly changed as it can be seen in the following:

- ➢ 10% hematite (Fe_2O_3), average crystallite size: 123 nm
- ➢ 22% magnetite (Fe_3O_4), average crystallite size: 82 nm
- ➢ 65% M-type Ba-hexaferrite ($BaFe_{12}O_{19}$), average crystallite size: 43 nm
- ➢ 3% W-type Ba-hexaferrite ($BaNiZnFe_{16}O_{27}$), average crystallite size: 165 nm

The homogenization was followed by the greenbody forming in magnetic field and final sintering. The greenbody forming was made by a 100 tonn hydraulic press with the help of the employees of TKI-ferrit, in the appropriate size press die, with 1 t/cm^2 pressure, for ~20 seconds, in a magnetic field about 6,5 kOe. The final sintering was at 1300 ^{o}C temperature, in oxygen flow, for 4 hours, also at TKI-ferrit. The phase composition and the crystal phase clearness of the produced material was also proved by X-ray diffractional analysis.

Based on the diffractogram of figure 3.16. it can be stated that the produced W-type hexaferrite is nearly clean, contains only 3% M-hexaferrite phase. Besides this there were no other iron containing oxides and no other cristallized or amorphous components. The cristallite size of the W-hexaferrite was 247 nm.
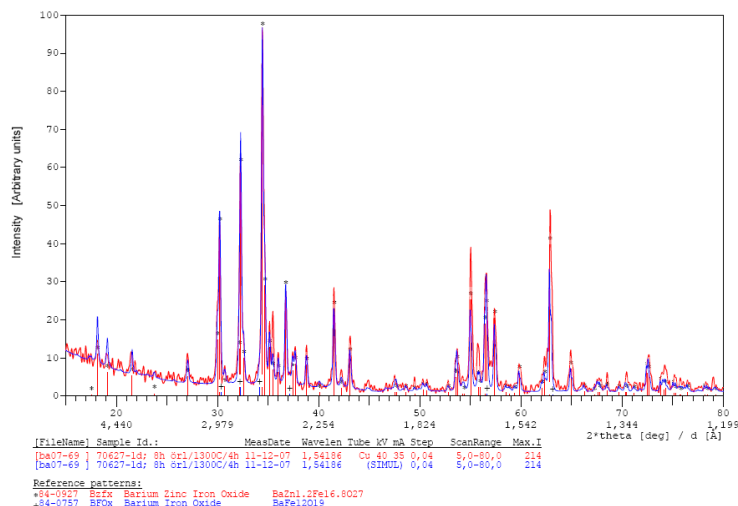

Figure 3.16. The X-ray diffraction pattern of the end product

According to the morphological tests by scanning electron microscope (SEM) it can be determined that the shape of the grains of the produced material are hexagonal. The cristals have representative morphology, they are plate shaped and orthogonal to the direction of c-axis the size of most of them is about 200 nm. The other sizes of the cristallite plates are about a few hundred nanometers (~225-400 nm). The nanocrystallite sizes determined by XRD test are almost the same to the c-axis. The scanning electron microscope picture of the end product can be seen on figure 3.17. According to the picture it can be determined that the greenbody forming of these fine powders in magnetic field is not solved, while we did not get solid structure. So, the further optimization of the forming in magnetic field as an important technological step during the production of hexaferrite is reasonable.
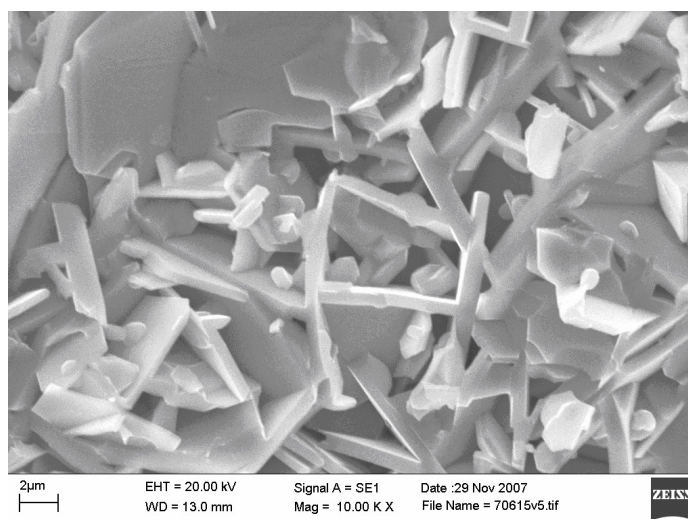

Figure 3.17. The SEM micrograph of the end product

I have examined the magnetic and microwave parameters of the produced W-type Ba-hexaferrite end product. I have examined the results of the Vibrating Sample Magnetometer (VSM) tests in two ways (easy and heavy magnetizing direction). The magnetizing curve that shows the results of the tests can be seen on figure 3.18. The calculated magnetic characteristics from the measurements:

> saturation magnetization: $M_s = 0{,}46$ T

> anisotropy constant: $K_1 = 9{,}3$ kJ/m^3

> coercivity: $H_c = 40560$ A/m
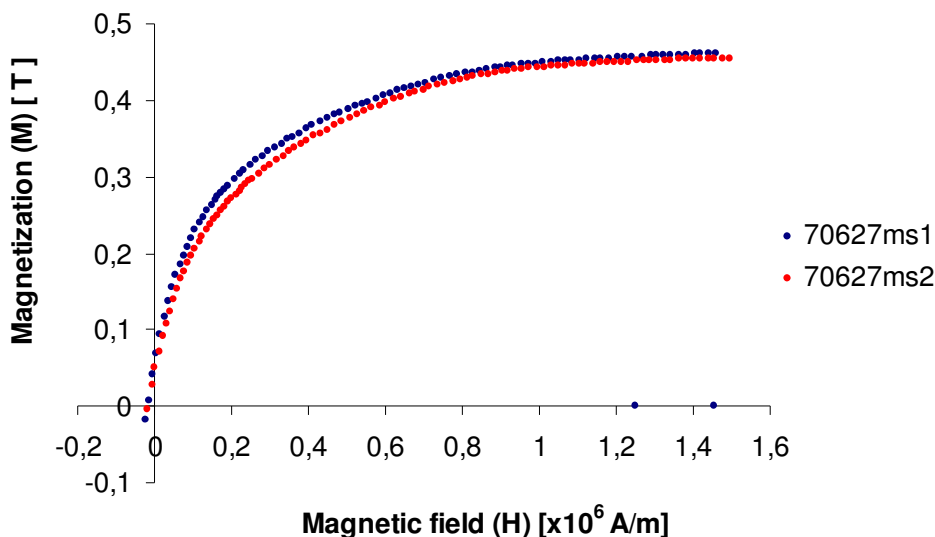
Figure 3.18. The result of the magnetic measurement of the end product (70627ms1: easy magnetizing direction (parallel to the anisotropy space), 70627ms2: hard magnetizing direction (perpendicularto the anisotropy space))

For the measuring of the dielectric characters of the end product I applied the measuring device of the BME Chair of Microwave. We have executed the tests on different frequencies and determined the dielectric constant of the end (ε) and it's losses (tg δ). The table 3.2. shows the measured values of the end product. From the table the dependence on the frequency of the dielectric constant and dielectric losses can be seen.

Table 3.2. The dependence on the frequency of the dielectric constant (ε) and the dielectric losses (tg δ)

frequency [GHz]	ε [F/m]	tg δ
8,7688	11,8635	0,0001
11,7016	12,7301	0,0002
14,1224	12,5581	0,0014
17,4500	14,4130	0,0021
18,9733	11,4958	0,0011
21,6010	12,1340	0,0034
24,4906	12,7242	0,0156

3.3. New scientific results

According to the researches of the milling process in planetary ball mill, my results are the following:

Thesis 1.: Applying the laws of motion of the classical mechanics I have set up a realistic, kinetic model to planetary ball mills. I have formulated common equations between the technological parameters of milling and the getting energy and output, under given boundary conditions, considering the dimensions of the milling ball.

Thesis 2.: I have determined those commonly usable curves ($E_b(i)$, $P(i)$), that help to indicate optimal combination of the milling parameters (n_p, i) and the milling energy in the Fritsch Pulverisette P4 planetary ball mill.

Thesis 3.: With the new method, I have determined the optimal milling parameters (n_p=400 rpm, n_v=800 rpm, i=2) to the present planetary ball mill (Fritsch Pulverisette P4) and the milling set (80 ml stainless steel vial and d_b=Ø10 mm, N_b=25 pcs balls) for the milling of the $Ba(Zn_{0.5}Ni_{0.5})_2Fe_{16}O_{27}$ chemical composition, m_p=20 g quantity W-type Ba-hexaferrite ceramic material system.

According to the experiments of the production of W-type barium-hexaferrite by high energy milling I have come to the following statements:

Thesis 4.: With the milling experiments I have shown that the milling of the raw materials (Fe_2O_3, ZnO, $NiCO_3$, $BaCO_3$) in different times and combinations did not bring the advantages in the formation of the solid phase reaction, that could be seen when milling all of the components together. The milling of all of the components at one time brings the best result.

Thesis 5.: I could produce W-type Ba-hexaferrite with a chemical composition $Ba(Zn_{0.5}Ni_{0.5})_2Fe_{16}O_{27}$ by a method based on the conventional production technology of hexaferrites with milling in a high energy planetary ball mill.

Thesis 6.: I have introduced a new additive (oleic acid) to the high energy milling of hexaferrite powders and I have proved the positive effects of it through the dry milling of the given material system in planetary ball mill. By milling with oleic acid additive, the result was smaller grain size, higher phase-purity in the sintered end product and it eliminated the usage of the organic liquid medium (acetone) that was used in the conventional process and was harmful to the environment.

4. CONCLUSIONS, SUGGESTIONS

According to my research, in the followings I summarize the correlations that extend our knowledge and can be helpful at the practical applications.

The examination of the milling process of the planetary ball mill led to the deductions, written below:

➢ I have set up a calculation method with which the delivered energy to the dust particles during the impact of the milling ball and the output of the milling can be determined in case of any kind of planetary ball mills at given conditions.

➢ Knowing the impacting energy, a so-called milling map can be drawn, and with the help of it, the amount of energy can be determined in advance with which the required phase can be reached in case of mechanical milling.

➢ The experimental results pointed that the hexaferite powder produced with high energy milling can not only be used to form blocks of materials, but it also can be used for thick layer technology of printed-circuit boards. A technological line that is combined with this method, it is possible to produce ferrite dust, from which self magnetizing, very little sized (few millimetres) ferrite devices can be produced with lithographic methods for thick layer electrical circuits.

Based on my research, my suggestion for further researching areas are the following:

➢ During the modelling of the planetary ball mills, I have fixed as a boundary condition that I neglect the decelerating effect of the grain, when determining the impact speed. As a future task, it would worth to examine the effect of a certain grain loaded in a greater amount to the change of the impact speed that could make the determination of the delivered energy to the dust particles during the impact more precise.

➢ My calculation model is true in case of dry milling. Although in practice because of certain technological reasons, they apply millings in liquid medium too (to decrease dusting) for producing different materials. As a future task, a modified model should be found, that would allow the determination of the delivered energy in case of millings applied in liquid medium.

➢ The revision and further optimalization of the process and the different technological steps of the production of the W-type Ba-hexaferrite by high energy mechanical milling would probably lead to an end product with better magnetic and dielectric characteristics. The end product shown on Figure 3.17. is a very porous material, that causes bad magnetic characteristics. To improve the solidity of the product, the development of the method of moulding in magnetic field technology would be required. However, according to the program of the TKI-Ferrit Kft. this task can only be examined in a subsequent research project.

5. SUMMARY

The mechanical milling is a common method for producing fine material that is used for decades. The high energy mechanical milling gives a great opportunity for the researching and developing experts for producing new and more advantageous materials (for example nanostructured materials, amorphous-, quasi-crystalline-, crystalline metastable alloys). A great group of the magnetic ceramics can also be listed here because of their advantageous magnetic character and also hexaferrites that are often applied in several communication electronics devices. Although the dynamic improvement of telecommunication needs the size reduction of the devices that contain ferrite and the ferrite materials that are inside them that leads to the increased importance of the chemical and morphological homogeneity in the material. The new requirements can't be fulfilled with the classical ceramic technologies, but placing the high energy mechanical milling in the technological line it becomes possible to create the required characteristics. High energy mechanical milling can be implemented in several devices that work different ways, but the most widespread method among the researchers is the planetary ball mill. The controllability and designability of the grinding procedure needs the accurate understanding and discovering of the interaction between the parameters that affect the milling and the delivered energy to the grinds.

In the first part of my thesis I determined the main factors of the milling in case of a planetary ball mill that affects the efficiency of the grinding (kinetic energy) and can be the controlling parameters of the method. Parallel to this, I developed a calculation model for determining the milling energy that is mathematically common and it can simulate the grinding method of the planetary ball mill at given conditions. In the second part of my thesis I write down the milling experiments I have made. The goals of the experimens were to create a type of a ceramic material system, the W-type Ba-hexaferrite. I have checked the technological changings of each step by using modern material testing methods.

During the reading of the professional literature, I have processed more than a hundred, mostly foreign scientific publications. I have summarized the manufacturing processes of the nanostructure materials, mainly the nanopowders, with a special focus on the mechanical milling; the characteristics of the hexaferrites and the experiments for their creation and the results that are reached so far in the field of the modeling of the planetary ball mills. At the end I have rated these methods. In the end of the chapter I have named the deficiencies of the given field and listed the problems that should be solved.

I have formulated a calculation method for planetary ball mills to determine the transferred influence energy and output. I have found correlations between ratio of the speed of the main disc and the vials and the geometric parameters of the mill. Based on the rsults of the calculations I have determined the required parameters for the grinding of hexaferrites and have done experiments.

During the milling experiments first I have done the premilling experiments of the base materials (Fe_2O_3, ZnO, $NiCO_3$, $BaCO_3$). With the set parameters I could reach crystallite size less than 100 nanometer during the millings. In the second phase of the experiments I have done millings in different medium (ethanol, distilled water, acetone) and also with additive (oleic acid) and studied the effect of these materials on milling and the further technological steps of the production of W-type Ba-hexaferrite. After the finishing of the experiments I could show that from the used additives that were used to help the milling, the best was the oleic acid. By using oleic acid the agglomeration of the dust particles is blocked, it reduces the abrasion of the milling set (vial and balls) and last, but not least this additive is ecologically beneficial, because it is effective at a very low amount (0,2 mass percent). In the final part of my research I have partly modified the classical ceramic technology (used high energy ball milling instead of low energy ball milling and applied lower sintering temperature). With these I could produce W-type barium-hexaferrite. I have featured the structural, morphological, magnetic and dielectric characteristics of the produced material and fully documented the producing procedure.

According to my examinations I have formulated my new scientific results that are summarized in an individual thesis booklet. At last I have made suggestions for the empirical usage of the results and for further research tasks.

By developing the correlation between the created model of the grinding process in the planetary ball mill and the milling parameters; and by the results of the completed calculations we could get new information about the delivered energies to the grinds and the efficiency of milling. The discovered new information lead to a more designable mechanical milling for the experts who develop production technologies and research materials and the process also opens new ways for different applications in case of factual ceramic materials.

6. PUBLICATIONS IN CONNECTION WITH THE THEME OF DOCTORAL DISSERTATION

Periodical articles:

- In foreign languages with impact factor:

[1]   I. ZSOLDOS, **GY. KAKUK** et al. (2004): Geometric construction of carbon nanotube junctions, *Modelling and Simulation in Material Science and Engineering*, 12 1251-1266. p.
Citations:
Graovac A., László I., Pisanski T.: *Match* 60 (3) 917-926. p., 2008
Qin Z., Feng X.Q., Zou J. et al.: *J. Nanosci. and Nanotech.* 8 (12) 6274-6282. p. 2008
Laszlo I.: *Croatica Chem. Acta* 81 (2) 267-272. p. 2008
Kyoko Nakada et al.: *J. Math. Chem.* 2008, DOI 10.1007/S10910-008-9419-Y
Laszlo I.: *Solid State Phys.* 244 (11) 4265-4268 p. 2007
Tasci E, Erkoc S.: *J. Nanosci. and Nanotech.* 7 (4-5) 1653-1661 p. 2007
Coluci V.R. et. al.: *Phys. Rev.* B 75 (7) Art. No. 075417 Feb 2007
Tasci E: Ph.D. thesis, *The Grad. School of Nat. and Appl. Sci. of Mid. East Tech. Univ.,* Ankara, 2007
Coluci V.R. et al.: *Nanotech.* 17 (3) 617-622. p. 2006
Laszlo I.: *Solid State Phys.* 243 (13) 3468-3471 p. 2006
Coluci V.R. et al.: *Ma. Res. Society Symp. Proc.* 963 1-6. p. 2006

[2]   I. ZSOLDOS, **GY. KAKUK** et al. (2005): Set of Carbon Nanotube Junctions, *Diamond and Related Materials*, 14 (3-7) 763-765. p.
Citations:
Graovac A., László I., Pisanski T.: *Match* 60 (3) 917-926. p., 2008
Laszlo I.: *Croatica Chem. Acta* 81 (2) 267-272. p. 2008
D. C. Wei, Y. Q. Liu: *Adv. Mat.* 20 (15) 2815-2841. p. 2008
Kyoko Nakada et al.: *J. Math. Chem.* 2008, DOI 10.1007/S10910-008-9419-Y
Laszlo I.: *Solid State Phys.* 244 (11) 4265-4268 p. 2007
Tasci E, Erkoc S.: *J. Nanosci. and Nanotech.* 7 (4-5) 1653-1661 p. 2007
Tasci E: Ph.D. thesis, *The Grad. School of Nat. and Appl. Sci. of Mid. East Tech. Univ.,* Ankara, 2007
Laszlo I.: *Solid State Phys.* 243 (13) 3468-3471 p. 2006

[3]   T. PATAKI, **GY. KAKUK**, I. ZSOLDOS (2007): Dynamical Behaviour of Carbon Nanotubes, *Diamond and Related Materials*, 16. 288-291. p.

[4]   Á. CSANÁDY, L. IPACS, **GY. KAKUK** et al. (2007): Characterization and comparison of rapidly solidified Al particles, mechanically milled nanostructures and their consolidated structures made by high energy rate forming technology (HERF), *Material Science Forum,* 537-538 321-328. p.

[5]   I. ZSOLDOS, **GY. KAKUK** (2007): New formations of carbon nanotube junctions, *Modelling and Simulation in Materials Science and Engineering* 15 1–7. p.
Citations:
D. C. Wei, Y. Q. Liu: *Adv. Mat.* 20 (15) 2815-2841. p. 2008
Velmre E. et al.: *International Biennial Baltic Electronics Conf., Proc.75-78. p. 2008*

[6]   **GY. KAKUK**, A. CSANADY et al. (2008): The influence of nanomilling on the formation of Ba- hexaferrite, *Reviews on Advanced Materials Science*, 4 (18) 317-321. p.

[7]   **GY. KAKUK,** Á. CSANÁDY et al. (2008): The influence of high-energy ball milling parameters on the traditional W-type Ba-hexaferrite properties, *Material Science Forum*, 589 397-402. p.

[8]   SZ. HERCZEG, J. TAKÁCS, Á. CSANÁDY, **GY. KAKUK** et al. (2008): Solid-state transformation produced by laser tratment and mechanical alloying of Fe-Ni-Cu(P) powders, *Material Science Forum*, 589 391-396. p.

[9] **GY. KAKUK** et al. (2009): The modelling of the milling process in a planetary ball mill, *Modelling and Simulation in Materials Science and Engineering*, Ref: MSMS/310854/PAP/225011, under publishing

- Opposed article in Hungarian languange:

[10] **KAKUK GY.,** CSANÁDY Á. (2006): Nanoszerkezetű anyagok előállítása mechanikai őrléssel, *Gép*, LVII. évf. 1. szám, 24-28. p.

[11] **KAKUK GY.**, ZSOLDOS I., CSANÁDY Á., OLDAL I. (2009): Bolygó golyósmalom őrlési folyamatának vizsgálata I.: kinematikai és kinetikai modellezés, Gépgyártás, under publishing

[12] **KAKUK GY.**, ZSOLDOS I., CSANÁDY Á., OLDAL I. (2009): Bolygó golyósmalom őrlési folyamatának vizsgálata II.: behatási energia és őrlési teljesítmény optimálása, Gépgyártás, under publishing

Conference proceedings:

- International conference proceedings:

[13] **GY. KAKUK**, A. CSANADY, L. TRIF, I. SAJÓ, A. SZTANISZLAV, E. KÁLMÁN, A. VÉRTES (2007): The effect of mechanical milling on the formation of W-type Ba-hexaferrite, 18th International Conference on Electromagnetic Fields and Materials, Budapest, 17-18 May, 2007.

- Hungarian conference proceedings:

[14] ZSOLDOS, I., **KAKUK, GY.** (2005): Szén nanocső elágazások rendszere, XXIX. Kutatási és Fejlesztési Tanácskozás, Gödöllő, 2005. január 18 -19.

- International conference abstract:

[15] I. ZSOLDOS, **GY. KAKUK** (2005): New formations of carbon nanotube junctions, 5th Hungarian Materials Science Conference, 9th - 11st October 2005, Balatonfüred

[16] **GY. KAKUK**, Á. CSANADY, L. TRIF, I. SAJÓ, K. PAPP, A. SZTANISZLAV, E. KÁLMÁN (2006): The influence of nanomilling on the formation of Ba- hexaferrite, International Symposium on Metastable and Nano Materials, 27th - 31st August 2006, Warsaw, Poland

[17] **GY. KAKUK**, A. CSANADY, L. TRIF, I. SAJÓ, A. SZTANISZLAV, E. KÁLMÁN (2006): The effect of nanomilling on the formation of Ba-hexaferrite, Inorganic Materials, 23rd - 26th September 2006, Slovenia, Ljubljana

[18] **GY. KAKUK** et al. (2006): The study of W-type Ba-hexaferrite production by nanomilling and sol-gel route, HUNN - Hungarian Network of Excellent Centres on Nanosciences, Tecnology Transfer Day, 16 October 2006, Miskolc

[19] **GY. KAKUK** et al. (2007): The Effect of High-energy Mechanical Milling and Heat Treatment on the Formation of W-type Hexaferrite, HUNN - Hungarian Network of Excellent Centres on Nanosciences, Tecnology Transfer Day, 11 October 2007, Budapest

[20] **GY. KAKUK** et al. (2007): The Effect of High-energy Mechanical Milling and Heat Treatment on the Formation of W-type Hexaferrite, 6th Hungarian Materials Science Conference, 14th - 16st October 2007, Siófok

[21] SZ. HERCZEG, J. TAKÁCS, Á. CSANÁDY, **GY. KAKUK** et al. (2007): Solid-state Reactions Produced by Laser Tratment and Mechanical Alloying of Fe-Ni-Cu(P) Powders, 6th Hungarian Materials Science Conference, 14th - 16st October 2007, Siófok

- Hungarian conference abstract:

[22] **KAKUK, GY.,** TRIF, L., SAJÓ, I., CSANÁDY, Á., SZTANISZLÁV, A., KÁLMÁN, E., VÉRTES, A. (2006): W-típusú Ba- hexaferrit előállítása nanoőrléssel és szol-gél eljárással, HUNN - Hungarian Network of Excellent Centres on Nanosciences, Technológiai Tudástranszfer Napja, 2006. 10. 16.

[23] **KAKUK GY.**, CSANÁDY Á. et al. (2007): Nagyenergiájú mechanikai őrlés és hőkezelés hatása W-típusú hexaferrit kialakulására, HUNN - Hungarian Network of Excellent Centres on Nanosciences, Technológiai Tudástranszfer Napja, 2007. 10. 11.

Research reports:

[24] **KAKUK GY.** (2005): Hexaferritek előállítása nanotechnológiai módszerekkel (nagyenergiájú mechanikai őrléssel), (1. részjelentés), (társszerző) (Szerk.: Sztaniszláv A.) NKTH nyilvántartási szám: NKFP-3A/0004/2004

[25] **KAKUK GY.** (2006): Hexaferritek előállítása nagyenergiájú mechanikai őrléssel), (2. részjelentés), (társszerző) (Szerk.: Sztaniszláv A.) NKTH nyilvántartási szám: NKFP-3A/0004/2004

[26] **KAKUK GY.** (2007): Hexaferritek előállítása nagyenergiájú mechanikai őrléssel, technológia dokumentálása), (zárójelentés), (társszerző) (Szerk.: Sztaniszláv A.) NKTH nyilvántartási szám: NKFP-3A/0004/2004